MAE 440 - Aerodynamics Laboratory

Experimental Comparison of Drag of a Golf Ball with a Smooth Ball

Group Project

Niels Fuglede, 006020779
Kay Gemba, 003678517
Senad Bekiragik, 002519073
Yosihiro Tsumura, 004424847
Group 4

California State University
Department of Mechanical and Aerospace Engineering

MAE 440 - Aerodynamics Laboratory
Instructor: Rahai, Hamid R.
May 20, 2007

Abstract

The subject of aerodynamics has gained importance in sports such as golf because it improves performance of the game due to careful aerodynamic design of its equipment. In this paper, the drag of a golf ball is compared to the drag of a smooth sphere with similar diameter. The goal is to understand concepts of laminar and turbulent flow around a blunt body and to measure differences in performance. Subject to the same flow conditions, two different experiments were conducted to measure the C_d of the rough and smooth sphere: circumferential pressure distribution and a force balance. Integration of C_p over the surface was conducted for two different Reynolds numbers: 13600 and 28000. Calculations revealed corresponding drag coefficients of 1.14 ± 0.3 and 1.23 ± 0.3 for the smooth sphere, 1.10 ± 0.3 and 1.01 ± 0.3 for the rough sphere, respectively. Therefore, results indicate that the performance of the golf ball is superior to the smooth sphere due to improved aerodynamic flow.

Contents

List of Figures

List of Tables

1 Objective of experiment

In this paper it is investigated experimentally how the surface roughness effects the drag on a sphere. It is examined how pressure varies around a sphere with a smooth and a rough surface (ping pong ball and golf ball) placed in a cross flow. The spheres are placed in the center of a wind-tunnel and two series of pressure measurements are taken around the body, both in the sub-critical Reynolds number regime.
From the acquired data the circumferential pressure is calculated and from these values the drag coefficient due the pressure distribution can be determined. To validate the drag coefficients, the drag coefficients are also determined using a one dimensional force balance. Comparison is made between the results from the two different freestream velocities and Reynolds number effects are discussed.

2 Theory

2.1 Background

Flow characteristics around a sphere can be identified from the circumferential pressure distribution. The pressure distribution is a function of Reynolds number.

$$Re_d = \frac{\rho U_\infty D}{\mu} = \frac{U_\infty D}{\nu} \tag{1}$$

The Reynolds number is the ratio of inertia forces to viscous forces. Also, as the Reynolds number increases, flow separates from the sphere and creates a pressure differential across the cylinder which causes a drag force. An ideal flow would have no flow separation and the viscosity is assumed to be zero, meaning zero drag force. However, in actuality, the viscosity of the fluid causes the flow to separate from the surface of the object creating a maximum pressure at the front, stagnation pressure. When the Reynolds number is high, but finite, the flow is often modelled by separating the flow into a thin region close to the surface where viscous effects are considered called the boundary layer and the otherwise the flow is assumed to be inviscid, [3].
When the flow is assumed inviscid the theoretical results of the calculation of drag gives that there is no net pressure drag on the sphere and the flow is assumed to smoothly flow around the sphere. In reality the viscosity causes the flow to separate from the surface and a turbulent wake with a negative pressure forms behind the cylinder. Therefore the flow is dominated by viscous effects and no inviscid flow model can predict the aerodynamics of such a flow. It is known that viscous forces are greater when the flow is turbulent rather than laminar, but in spite of that viscous drag accounts for only about 5% of the total drag, [5].
To summarize this, the drag force is almost entirely due to the pressure distribution and viscous forces can be neglected, but viscous effects are essential to explain the flow characteristics.
The pressure and drag coefficients are defined as follows:

$$C_p = \frac{p - p_\infty}{q_\infty} \tag{2}$$

where p_∞ is the freestream pressure and q_∞ is the dynamic pressure, defined as

$$q_\infty = \frac{1}{2}\rho_\infty V_\infty^2 \tag{3}$$

Here ρ_∞ and V_∞ is the density and velocity in the freestream far ahead of the body. Let dV/dy be defined as the velocity gradient at the surface and let μ be the viscosity of the fluid. Then the shear stress at the surface is given by

$$\tau = \mu \frac{dV}{dy} \tag{4}$$

Aerodynamic lift, drag and moments on a body can be found by integrating the pressure distribution, $p(s)$, and shear stress distribution, $\tau(s)$, over the body. Finding these distributions are often the major goal of theoretical and computational fluid dynamics. Because the drag force is acting in horizontal direction the drag coefficient due to pressure, $C_{d,p}$, can be found by integrating the horizontal component of the pressure coefficient distribution, that is

$$C_{d,p} = \frac{1}{2} \int_0^{2\pi} (C_p \cos\theta) \mathrm{d}\theta \tag{5}$$

The pressure is acting normal to the pressure and oriented the angle θ relative to the perpendicular, shear stress is tangential and oriented the same angle θ relative to the horizontal, as seen in Fig. 1.

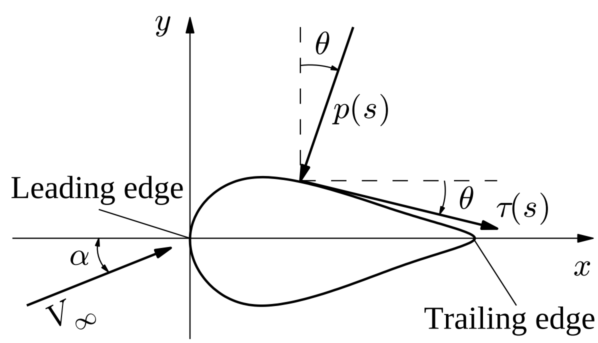

Figure 1: Nomenclature for pressure and shear stress distribution

2.2 Golf Ball Aerodynamics

The difference in the flowfields around a smooth sphere and a rough, or dimpled, sphere can be seen in Fig. 2. Since the laminar boundary layer around the smooth sphere separates so rapidly, it creates a very large wake over the entire rear face. This large wake maximizes the region of low pressure and, therefore, results in the maximum difference in pressure between the front and rear faces. This difference creates a large drag since the drag is a function of pressure and is the integral over the entire surface. The transition to a turbulent boundary layer, on the other hand, adds

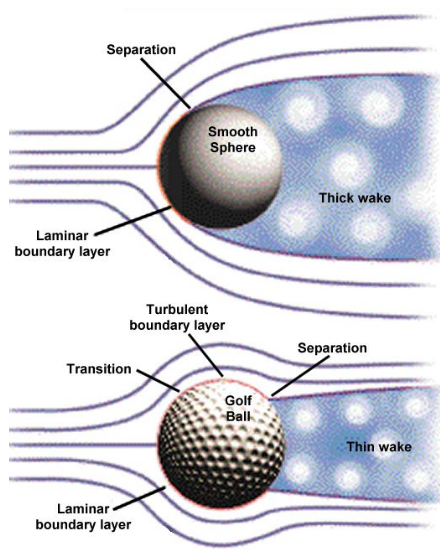

Figure 2: Viscous flow over a smooth Sphere and a Golf Ball, [1]

energy (momentum) to the flow allowing it to remain attached to the surface of the sphere further aft. Since separation is delayed, the resulting wake is much narrower. This thin wake reduces the low-pressure region on the rear face and reduces the difference in pressure between the front and back of the sphere. This smaller difference in pressure creates a smaller drag force comparable to that seen above the transition Reynolds number. The critical Reynolds number for a smooth sphere is found to about 3×10^5, corresponding to a usual diameter of a golf ball, [2]. In order for flow to be turbulent, the smooth ball would have to reach a speed of at least 110 ms^{-1}, which is unlikely. A solution is to use a dimpled sphere. It is found that the boundary layer for the dimpled ball becomes turbulent at 21 ms^{-1} corresponding to a critical Reynolds number of 6×10^4, [4].

3 Experimental procedure

3.1 Calibration of force balance

Calibration for measurement of the force is carried out by loading the one dimensional balance with different weights from 2 - 16 N and recording the output voltage of the load cell. A sketch of the setup is shown in Fig. 3.

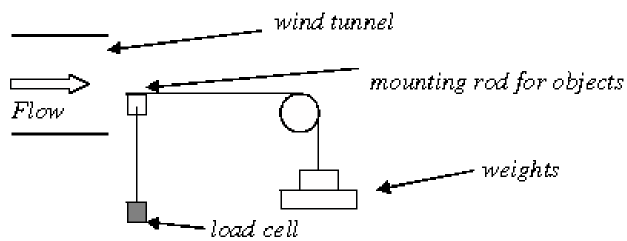

Figure 3: Setup for calibration of force balance

3.2 Pressure distribution

The spheres are mounted on a rod and placed in the center of the wind tunnel, and two series of measurements are carried out at two different freestream velocities. The rod is mounted on a device from a milling machine shop and rotates the spheres around the north-south axis. A pitot tube is mounted at a point on the equator from the inside of the sphere and another pitot is placed in the wind tunnel, measuring the total pressure. By using these two pressure measurements the differential pressure, Δp, is calculated directly and sampled by the equipment. To get the pressure distribution around the equator, the spheres are manually rotated in steps of $5\,^{\circ}$, until a full rotation is achieved. For every orientation 100 measurement of the pressure is sampled. Experimental setup is shown in Fig. 4.

3.3 One dimensional force balance

Measurements of drag are carried out behind the open end of a wind tunnel, with the spheres mounted on a one-dimensional balance. Measurements are taken at two different free stream velocities. Using the one-dimensional balance the drag force can be calculated using calibration-data and free stream velocity are calculated from the dynamic pressure. The dynamic pressure is measured using two pitot tubes measuring static and total pressure. Four measurements are taken for each sphere taken, with free stream velocity in the interval 12-25 m/s, at stabil readings for force and dynamic pressure, [5].

4 Experimental data

4.1 Calibration data

The results from the calibration of the one dimensional balance are listed in table 1.

Load [Newton]	2.6387	7.0884	11.5382	15.9879
Output [Volt]	0.2090	0.6730	1.2200	1.4670

Table 1: Data from calibration of one dimensional balance

4.2 Pressure distribution data

The data acquired for all the measurements are listed in table A.1. The data listed in the table includes the mean differential pressure, $\Delta\bar{p}$, local pressure coefficient θ_i, local drag contribution and

(a) Golf ball mounted in windtunnel

(b) Device used to rotate golf ball

Figure 4: Experimental setup and test objects

the local error in $\Delta\bar{p}$.

4.3 Drag force results

The results from measurements of drag force using the one dimensional balance are listed in table 2 for the smooth sphere and in table 3 for the rough sphere.

Output [Volt]	0.050	0.110	0.168	0.173
$\Delta\bar{p}$ [in of H_2O]	0.409	0.744	1.181	1.726

Table 2: Data from measurement of drag force on smooth sphere

Output [Volt]	0.063	0.113	0.160	0.166
$\Delta\bar{p}$ [in of H_2O]	0.413	0.746	1.187	1.728

Table 3: Data from measurement of drag force on rough sphere

5 Calculations and experimental results

5.1 Calibration

The result of the calibration of the one dimensional balance is is shown in Fig. 5. To obtain a mathematical relationship between force and output voltage the data is fitted with a line, using least square method. The correlation coefficient of the linear fit is $R_1 = 0.9899$ and the plot of the measured values doesn't indicate any systematic deviation. Therefore the linear approximation is good and the slope of the line gives the relation $a_1 = 0.0971\ V/N$. When measurements are taken the equipment is used to zero the force output when the freestream velocity is zero.

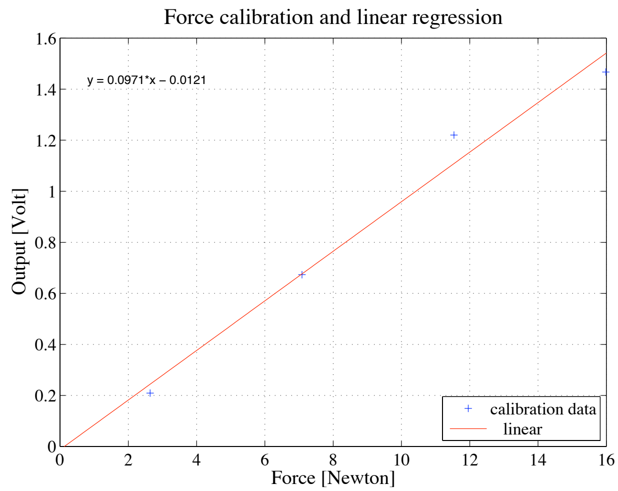

Figure 5: Linear regression on force calibration data

5.2 Pressure distribution

For every orientation 100 measurements of the pressure is taken. By calculating the mean pressure for every orientation, the mean pressure distribution, $\Delta\overline{p}_\theta$, is found. Freestream velocity is measured using the pitot tube in the cylinder oriented $0\,^\circ$ relative the freestream velocity, which is also known as the stagnation pressure, $\Delta\overline{p}_0$. Using the Bernoulli equation the velocity can be found from the measurement of stagnation pressure using

$$\overline{V} = \sqrt{2\rho\Delta\overline{p}_0} \tag{6}$$

When $\Delta\overline{p}$ is measured in inches of water the freestream velocity given in m/s at standard conditions can be found from

$$\overline{V}_\infty = 19.61\sqrt{\Delta\overline{p}_0} \tag{7}$$

Using (2) the mean circumferential pressure distribution is given by

$$C_p(\theta) = \frac{\Delta\overline{p}_\theta - \Delta\overline{p}_0}{\Delta\overline{p}_0} \tag{8}$$

When $C_p(\theta)$ is calculated, the drag coeffecient can be estimated using (5) in the discrete form

$$C_d = \frac{1}{2}\sum_{\theta=0}^{2\pi} C_p(\theta)\cos(\theta)\frac{2\pi}{72} \tag{9}$$

Using the equations above the C_p can be shown as a function of θ and the results for the two series are shown in Fig. 6. The complete list of experimental results are shown in table A.1. The drag coefficients are listed in table 4. The two pressure distributions for the smooth sphere are shown in Fig. 7(a) and for the rough sphere in Fig. 7(b).

Sphere	Re	C_d
Smooth	13591	1.14
Rough	14137	1.10
Smooth	27702	1.23
Rough	27886	1.01

Table 4: Data from measurement of pressure distribution

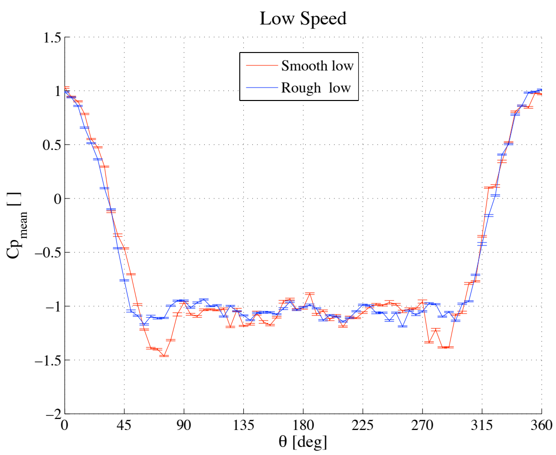

(a) Reynolds number ≃ 13600

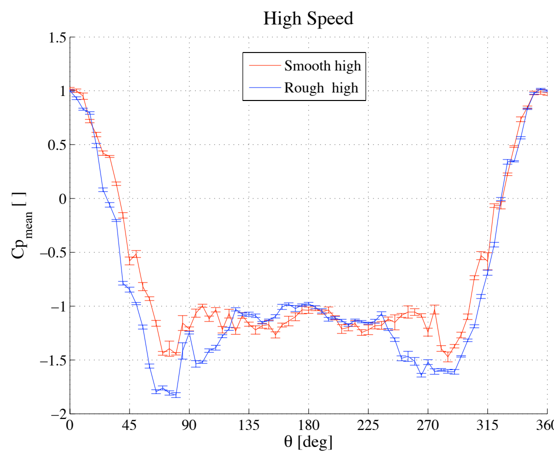

(b) Reynolds number ≃ 28000

Figure 6: Pressure coefficient around the smooth and rough sphere with uncertainty intervals

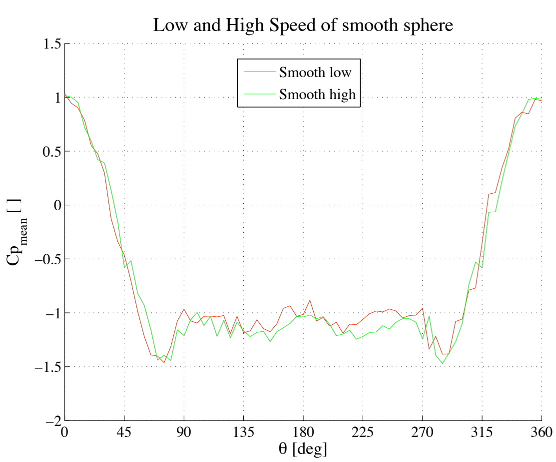

(a) Pressure distribution on smooth sphere

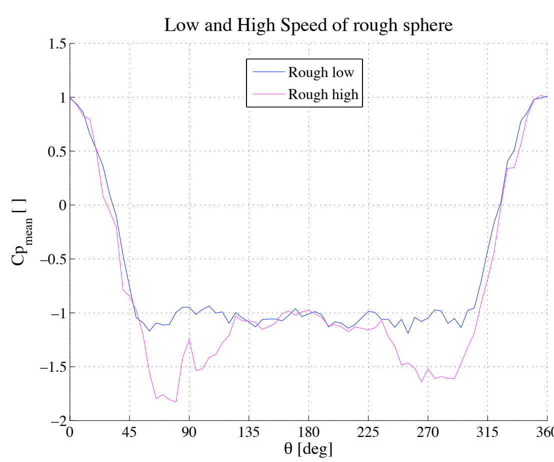

(b) Pressure distribution on rough sphere

Figure 7: Pressure distribution as a function of Reynolds number for smooth and rough sphere

5.3 Drag from one dimensional balance

To determine the drag coefficients from the force balance measurements listed in table 2 and 3 the following calculations are done. The drag force is determined using the calibration constant $a_1 = 0.0971\ V/N$

$$F_i = \frac{1}{a_1} W_i \tag{10}$$

where W_i is the output voltage from the measurements. Velocity is calculated from the differential pressure as

$$V_i = 19.61\sqrt{\Delta p_i} \tag{11}$$

Knowing the velocity, the Reynolds number is given by

$$Re_i = \frac{dV_{0,i}}{\nu} \tag{12}$$

Here, $d = 1.5''$ is the diameter of the spheres and $V_{0,i}$ is the free stream velocity calculted from the stagnation pressure. The drag coefficient is then given as

$$C_{d,i} = \frac{F_i}{\frac{1}{2}\rho V_{0,i}^2 A} \tag{13}$$

where $A = \pi d^2/4$ is the projected area of the sphere. The result of these calculations are shown in figure 8.

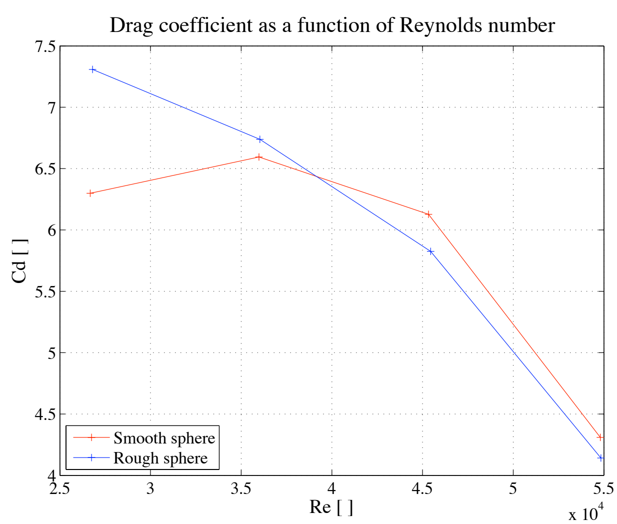

Figure 8: Drag force on smooth and rough sphere as a function of Reynolds number

6 Uncertainty analysis and errors

6.1 Uncertainty values

In order to get a confidence interval of 95%, the error around the mean is calculated from the raw data, and multiplied by a factor of 2, according to (14). For all 73 intervals, and for each Reynolds number, the maximum of these intervals is chosen to be the confidence interval.

$$CI = 2\sigma = \frac{1}{n-1}\sqrt{\sum_{i=1}^{n}(x_i - \overline{x})^2} \tag{14}$$

Table 5: Calculated Uncertainties

ΔP Pitot Tube	$\pm 0.004\ in - H^2O$
D	$\pm 0.005\ in$
U_∞	$\pm 0.63\ m/s$
ΔP Ball	$\pm 0.02\ in - H^2O$
C_P	± 0.028
C_D	± 0.03
Re	± 0.7

6.2 Sample Calculation

The different uncertainty values are calculated from the expression listed below

$$C_d = f\left(\sum C_p, \sum cos\theta\Delta\theta\right)$$

$$U_{C_d} = \pm\left[\left(\frac{\sum C_p}{C_d}\frac{\partial C_d}{\partial \sum C_p}U_{\sum C_p}\right)^2 + \left(\frac{\sum cos\theta\Delta\theta}{C_d}\frac{\partial C_d}{\partial \sum cos\theta\Delta\theta}U_{\sum cos\theta\Delta\theta}\right)^2\right]^{\frac{1}{2}}$$

$$U_{C_d} = [U^2_{\sum C_p} + U^2_{\sum cos\theta\Delta\theta}]^{\frac{1}{2}}$$

$$U_{\sum cos\theta\,\Delta\theta} = \sum cos(\frac{\pi}{4*180}) = 0.0087$$

$$U_{\sum C_p} = \pm 0.007$$

$$U_{C_d} = [(U_{\sum C_P})^2 + (U_{\sum cos\theta\,\Delta\theta})^2]^{\frac{1}{2}} = .03$$

7 Discussion of results

Discussion of results are most easily done considering the Bernoulli equation in the form

$$p + \frac{1}{2}\rho V^2 = \text{Constant} \tag{15}$$

As a general result from the experiments, it can be seen that the velocity at the surface of each sphere and the local static pressure are both functions of Reynolds number and rotation angle, θ. Once the pressure distributions have been found the pressure coefficient and the drag coefficient can be found. The pressure coefficient distribution in sub-critical Reynolds number fields remains essentially unchanged.

The drag coefficients for both speeds are slightly higher than 1. For the higher Reynolds number it is found to be 1 for the rough sphere and 1.2 for the smooth sphere.

The mean pressure differences plotted as a function of rotation angle, θ, can be seen in Fig. 7(a) and in Fig. 7(b) as a direct comparison for each sphere. The fluid hits each sphere at the stagnation point, $\theta = 0\,^{\circ}$, and will have zero velocity and hence maximum pressure will be exerted on the sphere. As θ increases, the flow will have a higher velocity and the Bernoulli equation dictates a lower pressure, which is also observed in the experimental results.

Theoretically, the pressure distribution should be symmetrical around a vertical line at $\theta = 180°$. By looking at the figures 6 and 7, this is almost the case but some variation can be observed, which is most likely due to the discrete distribution of the measuring points. For the smooth sphere, the fluid is accelerated and has maximum velocity at around 70° and at 290°. Afterwards, the flow decelerates and is separates at around 90° and 270°. In the back of the sphere, pressure remains almost constant, neglecting slight variations. Because the speed and the calculated Reynolds numbers are in the sub-critical regime, the boundary layer was found to be laminar. As mentioned in the golf ball aerodynamics theory, section 2.2, a Reynolds number of 3×10^5 is needed for the flow to become turbulent for smooth spheres. Notice that both pressure distributions for the smooth ball in Fig. 7(a) are essentially the same, meaning similar drag for both Reynolds numbers. Our results find this to be true. Drag coefficients are calculated to be 1.137 and 1.2264 for low and high speed, respectively. This is a value slightly higher than what was expected, [3]. The difference can be explained by the setup of this experiment. The ball was mounted on a cylinder, which is a source of drag, too.

The pressure distribution for the rough sphere in Fig. 7(b) is also very symmetrical about the center. However, the plots for the rough sphere vary as a function of Reynolds number differently then the smooth sphere. For the lower velocity, separation of the fluid is found to be at roughly 60° and 300°. The point of separation is roughly equal to the point of maximum velocity. Now, as velocity increases, the flow is found to be attached longer to the sphere. For the higher Reynolds number, separation occurs at 130° and 230°. It seems that the flow around the golf ball starts to become turbulent which agrees with the critical Reynolds number for rough spheres. Note that the negative pressure of the rough sphere approaches the value of the smooth sphere in the back of the ball later. However, it is problematic comparing these two speeds since one is laminar and the 2nd one in transition to turbulent. The higher velocity introduced a later separation but the minima of the coefficient of pressure is lower than at low speed. As a result, the drag would be increased due to a bigger net pressure due to the negative region. However, the curve in the positive region is much steeper. These results seem to indicate that the net pressure is actually reduced further as Reynolds number increases. Since the only thing which changed between the two objects is the surface roughness, this has to be the cause for the behavior of the flow. Calculated coefficients of drag are 1.1013 and 1.0084 for low and high speed, respectively. Both results are lower compared to the ones found for the smooth sphere. Note that the drag actually decreases for higher Reynolds numbers for the golf ball. Therefore, it can also be concluded that the higher speed was conducted in the transition or turbulent regime.

Comparing both spheres at low, laminar flow speed as shown in Fig. 6(a), it is easy to see that both graphs are similar except for two conditions. The flow around the smooth sphere separates later and it has greater minima of the coefficient of pressure then the rough sphere. The later result indicates that the drag for the smooth ball is larger at this speed, which is found to be true comparing the coefficients of pressure.

The comparison, the higher speed is show in Fig. 6(b). Note that the profile for the smooth sphere is almost constant as discussed above. Also, the point of separation for the golf ball changed backwards and its curve is generally below the smooth sphere for all values. What this means is that flow is starting to become turbulent. For fully developed turbulent flow, the golf ball is therefore expected to have even a lower coefficient of drag. This will most likely happen at Reynolds numbers above 6×10^4 where the flow around the rough sphere is complectly turbulent.

When the experimental values of the drag coefficients obtained in the experiment are compared to values from the reference literature, they are found to be roughly accurate. Values typically observed are in the range of about one and values obtained in this experiment are approximately 1.1 to 1.2 for the smooth sphere. For the golf ball, literature states that values can reach as low as 0.3. However, the drag of a golf ball is also a function of its spin. This was not part of this experiment.

Mounting both objects to a calibrated force balance subject to four different freestream velocities, it has been found that the drag for the rough sphere is lower for higher Reynolds numbers. However, values shown in Appendix A.2 are not comparable with theoretical values but just two each other. The calibration was done for higher values of loading, and our drag forces are at much lower than the forces applied in the calibration. Calculations results in C_d values ranging from 4.1 to 7.3 as seen in figure 8.

8 Conclusions and recommendations

In this experiment, the drag of a golf ball with a rough surface was compared to a smooth ping pong ball of equal diameter. Testing was performed for two Reynolds numbers, $13,600$ and $28,000$. Circumferential pressure distribution was measured in order to calculate the drag on the objects. Values slightly higher than one were found for the smooth sphere, increasing with higher Reynolds number. Due to the rough surface of the golf ball, the drag coefficient decreased as the freestream velocity increased. Both values obtained are lower compared to the smooth object. It can be concluded that the golf ball has better aerodynamics then the sphere since drag is less.
The free stream velocities are limited by the capabilities of wind tunnel and we could not perform the experiment we actually intended. Freestream velocities as high as $30ms^{-1}$ would be excellent to show the superiority of the golf ball. Nevertheless, calculated values in this report show lower drag coefficients for the golf ball, though they are not as distinctly different as we had hoped.

References

[1] http://www.aerospaceweb.org/question/aerodynamics/q0215.shtml.

[2] E. Achenbach. Experiments on the flow past spheres at very high reynolds number. *Jnl. Fluid Mech.*, 54(565), 1972.

[3] J. D. Anderson. *Fundamentals of Aerodynamics*. McGraw-Hill, fourth edition, 2005.

[4] A. R. Penner. The physics of golf. *Rep. Prog. Phys. 66*, pages 131–171, 2002.

[5] H. R. Rahai. *MAE 440 - Aerodynamics Laboratory Experiment*. University Bookstore CSULB, 2007.

A Appendix

The different Matlab codes and

A.1 Experimental pressure distribution results in tabular form

Data for Smooth_low – Reynolds number = 13591.4999

theta [deg]	dp [in H2O]	cp []	cp*cos(th)d_th	dp +–[in H2O]
0	0.1045	1.0309	0.0900	0.0072
5	0.0957	0.9447	0.0821	0.0061
10	0.0914	0.9022	0.0775	0.0051
15	0.0796	0.7852	0.0662	0.0064
20	0.0560	0.5523	0.0453	0.0060
25	0.0482	0.4752	0.0376	0.0056
30	0.0300	0.2961	0.0224	0.0056
35	–0.0125	–0.1238	–0.0088	0.0089
40	–0.0345	–0.3404	–0.0228	0.0122
45	–0.0470	–0.4635	–0.0286	0.0063
50	–0.0713	–0.7036	–0.0395	0.0057
55	–0.0998	–0.9843	–0.0493	0.0083
60	–0.1234	–1.2175	–0.0531	0.0062
65	–0.1410	–1.3908	–0.0513	0.0081
70	–0.1419	–1.4006	–0.0418	0.0077
75	–0.1483	–1.4631	–0.0330	0.0061
80	–0.1334	–1.3161	–0.0199	0.0072
85	–0.1091	–1.0768	–0.0082	0.0156
90	–0.0979	–0.9664	–0.0000	0.0090
95	–0.1090	–1.0759	0.0082	0.0091
100	–0.1110	–1.0954	0.0166	0.0089
105	–0.1048	–1.0343	0.0234	0.0083
110	–0.1044	–1.0305	0.0308	0.0064
115	–0.1052	–1.0382	0.0383	0.0057
120	–0.1038	–1.0246	0.0447	0.0078
125	–0.1210	–1.1935	0.0597	0.0072
130	–0.1048	–1.0337	0.0580	0.0139
135	–0.1200	–1.1836	0.0730	0.0058
140	–0.1184	–1.1680	0.0781	0.0083
145	–0.1079	–1.0648	0.0761	0.0184
150	–0.1162	–1.1466	0.0867	0.0122
155	–0.1192	–1.1760	0.0930	0.0068
160	–0.1118	–1.1035	0.0905	0.0072
165	–0.0972	–0.9590	0.0808	0.0130
170	–0.0947	–0.9346	0.0803	0.0086
175	–0.1047	–1.0328	0.0898	0.0082
180	–0.1029	–1.0149	0.0886	0.0133
185	–0.0896	–0.8837	0.0768	0.0078
190	–0.1091	–1.0768	0.0925	0.0094
195	–0.1057	–1.0431	0.0879	0.0084
200	–0.1140	–1.1246	0.0922	0.0107
205	–0.1102	–1.0872	0.0860	0.0094
210	–0.1207	–1.1906	0.0900	0.0067

215	−0.1120	−1.1053	0.0790	0.0122
220	−0.1126	−1.1113	0.0743	0.0058
225	−0.1075	−1.0603	0.0654	0.0079
230	−0.1022	−1.0087	0.0566	0.0076
235	−0.0997	−0.9838	0.0492	0.0089
240	−0.1006	−0.9922	0.0433	0.0071
245	−0.0977	−0.9643	0.0356	0.0163
250	−0.0996	−0.9829	0.0293	0.0087
255	−0.1063	−1.0494	0.0237	0.0122
260	−0.1040	−1.0259	0.0155	0.0098
265	−0.1035	−1.0215	0.0078	0.0067
270	−0.0970	−0.9571	0.0000	0.0151
275	−0.1355	−1.3368	−0.0102	0.0061
280	−0.1235	−1.2184	−0.0185	0.0123
285	−0.1402	−1.3833	−0.0312	0.0058
290	−0.1401	−1.3823	−0.0413	0.0060
295	−0.1095	−1.0803	−0.0398	0.0069
300	−0.1072	−1.0579	−0.0462	0.0114
305	−0.0800	−0.7897	−0.0395	0.0096
310	−0.0780	−0.7697	−0.0432	0.0064
315	−0.0356	−0.3514	−0.0217	0.0076
320	0.0102	0.1006	0.0067	0.0062
325	0.0118	0.1161	0.0083	0.0124
330	0.0349	0.3444	0.0260	0.0119
335	0.0529	0.5223	0.0413	0.0059
340	0.0818	0.8068	0.0662	0.0066
345	0.0873	0.8611	0.0726	0.0056
350	0.0857	0.8461	0.0727	0.0082
355	0.0993	0.9803	0.0852	0.0064
360	0.0982	0.9691	0.0846	0.0061

Data for Rough__low − Reynolds number = 14137.7931

theta [deg]	dp [in H2O]	cp []	cp*cos(th)d_th	dp +−[in H2O]
0	0.1084	0.9886	0.0863	0.0057
5	0.1030	0.9391	0.0816	0.0051
10	0.0943	0.8595	0.0739	0.0060
15	0.0721	0.6576	0.0554	0.0064
20	0.0563	0.5139	0.0421	0.0058
25	0.0399	0.3637	0.0288	0.0057
30	0.0105	0.0957	0.0072	0.0058
35	−0.0110	−0.1006	−0.0072	0.0057
40	−0.0507	−0.4619	−0.0309	0.0057
45	−0.0834	−0.7607	−0.0469	0.0057
50	−0.1146	−1.0455	−0.0586	0.0102
55	−0.1194	−1.0892	−0.0545	0.0062
60	−0.1282	−1.1693	−0.0510	0.0071
65	−0.1200	−1.0944	−0.0404	0.0102
70	−0.1220	−1.1128	−0.0332	0.0071
75	−0.1216	−1.1093	−0.0251	0.0058
80	−0.1092	−0.9962	−0.0151	0.0063
85	−0.1042	−0.9500	−0.0072	0.0061
90	−0.1040	−0.9481	−0.0000	0.0059
95	−0.1112	−1.0141	0.0077	0.0067
100	−0.1061	−0.9675	0.0147	0.0069

105	−0.1029	−0.9381	0.0212	0.0060
110	−0.1097	−1.0006	0.0299	0.0057
115	−0.1088	−0.9918	0.0366	0.0067
120	−0.1203	−1.0967	0.0479	0.0056
125	−0.1094	−0.9974	0.0499	0.0058
130	−0.1149	−1.0474	0.0588	0.0060
135	−0.1191	−1.0863	0.0670	0.0052
140	−0.1240	−1.1305	0.0756	0.0056
145	−0.1166	−1.0630	0.0760	0.0066
150	−0.1160	−1.0576	0.0799	0.0096
155	−0.1160	−1.0576	0.0836	0.0068
160	−0.1180	−1.0757	0.0882	0.0057
165	−0.1123	−1.0238	0.0863	0.0086
170	−0.1053	−0.9599	0.0825	0.0075
175	−0.1135	−1.0355	0.0900	0.0061
180	−0.1107	−1.0098	0.0881	0.0065
185	−0.1084	−0.9884	0.0859	0.0080
190	−0.1119	−1.0201	0.0877	0.0054
195	−0.1240	−1.1312	0.0953	0.0066
200	−0.1189	−1.0840	0.0889	0.0063
205	−0.1204	−1.0977	0.0868	0.0061
210	−0.1254	−1.1434	0.0864	0.0055
215	−0.1216	−1.1089	0.0793	0.0057
220	−0.1149	−1.0474	0.0700	0.0058
225	−0.1083	−0.9875	0.0609	0.0062
230	−0.1091	−0.9948	0.0558	0.0070
235	−0.1165	−1.0625	0.0532	0.0085
240	−0.1163	−1.0603	0.0463	0.0059
245	−0.1244	−1.1341	0.0418	0.0077
250	−0.1163	−1.0608	0.0317	0.0062
255	−0.1303	−1.1886	0.0268	0.0055
260	−0.1143	−1.0424	0.0158	0.0068
265	−0.1184	−1.0802	0.0082	0.0087
270	−0.1150	−1.0486	0.0000	0.0059
275	−0.1068	−0.9743	−0.0074	0.0074
280	−0.1077	−0.9819	−0.0149	0.0058
285	−0.1203	−1.0975	−0.0248	0.0053
290	−0.1156	−1.0539	−0.0315	0.0058
295	−0.1245	−1.1358	−0.0419	0.0068
300	−0.1073	−0.9782	−0.0427	0.0069
305	−0.1048	−0.9553	−0.0478	0.0055
310	−0.0778	−0.7094	−0.0398	0.0061
315	−0.0463	−0.4225	−0.0261	0.0138
320	−0.0174	−0.1583	−0.0106	0.0095
325	0.0031	0.0281	0.0020	0.0069
330	0.0447	0.4078	0.0308	0.0054
335	0.0554	0.5055	0.0400	0.0066
340	0.0854	0.7788	0.0639	0.0063
345	0.0945	0.8618	0.0726	0.0056
350	0.1078	0.9832	0.0845	0.0055
355	0.1087	0.9911	0.0862	0.0061
360	0.1109	1.0114	0.0883	0.0051

```
Data for Smooth_high— Reynolds number = 27702.3314
```

```
theta [deg] dp [in H2O] cp [] cp*cos(th)d_th  dp +—[in H2O]
```

0	0.4284	1.0175	0.0888	0.0141
5	0.4215	1.0011	0.0870	0.0159
10	0.4002	0.9505	0.0817	0.0294
15	0.3027	0.7190	0.0606	0.0158
20	0.2499	0.5936	0.0487	0.0209
25	0.1772	0.4209	0.0333	0.0203
30	0.1642	0.3901	0.0295	0.0090
35	0.0578	0.1373	0.0098	0.0164
40	−0.0661	−0.1570	−0.0105	0.0253
45	−0.2444	−0.5804	−0.0358	0.0364
50	−0.2172	−0.5160	−0.0289	0.0321
55	−0.3448	−0.8189	−0.0410	0.0380
60	−0.3918	−0.9306	−0.0406	0.0173
65	−0.4883	−1.1598	−0.0428	0.0268
70	−0.6055	−1.4382	−0.0429	0.0173
75	−0.5874	−1.3953	−0.0315	0.0706
80	−0.6074	−1.4426	−0.0219	0.0112
85	−0.4872	−1.1572	−0.0088	0.0693
90	−0.5103	−1.2121	−0.0000	0.0186
95	−0.4483	−1.0649	0.0081	0.0376
100	−0.4192	−0.9957	0.0151	0.0142
105	−0.4705	−1.1175	0.0252	0.0253
110	−0.4351	−1.0335	0.0308	0.0203
115	−0.5132	−1.2190	0.0450	0.0303
120	−0.4504	−1.0698	0.0467	0.0403
125	−0.5187	−1.2320	0.0617	0.0302
130	−0.4573	−1.0862	0.0609	0.0263
135	−0.4916	−1.1677	0.0721	0.0191
140	−0.5143	−1.2216	0.0817	0.0385
145	−0.4978	−1.1824	0.0845	0.0224
150	−0.4934	−1.1719	0.0886	0.0404
155	−0.5336	−1.2673	0.1002	0.0288
160	−0.4950	−1.1757	0.0964	0.0179
165	−0.4793	−1.1383	0.0960	0.0448
170	−0.4627	−1.0990	0.0944	0.0368
175	−0.4358	−1.0350	0.0900	0.0360
180	−0.4370	−1.0379	0.0906	0.0293
185	−0.4293	−1.0198	0.0887	0.0225
190	−0.4441	−1.0549	0.0907	0.0200
195	−0.4361	−1.0359	0.0873	0.0279
200	−0.4667	−1.1085	0.0909	0.0190
205	−0.5104	−1.2122	0.0959	0.0410
210	−0.5045	−1.1984	0.0906	0.0310
215	−0.4889	−1.1612	0.0830	0.0279
220	−0.5242	−1.2452	0.0832	0.0267
225	−0.5136	−1.2199	0.0753	0.0449
230	−0.4983	−1.1834	0.0664	0.0281
235	−0.4962	−1.1786	0.0590	0.0361
240	−0.4712	−1.1192	0.0488	0.0178
245	−0.4844	−1.1506	0.0424	0.0695
250	−0.4573	−1.0861	0.0324	0.0177
255	−0.4440	−1.0545	0.0238	0.0566
260	−0.4443	−1.0552	0.0160	0.0310
265	−0.4576	−1.0869	0.0083	0.0159
270	−0.5227	−1.2415	0.0000	0.0367

275	−0.4342	−1.0314	−0.0078	0.0413
280	−0.5866	−1.3932	−0.0211	0.0266
285	−0.6196	−1.4717	−0.0332	0.0461
290	−0.5777	−1.3722	−0.0410	0.0163
295	−0.5339	−1.2682	−0.0468	0.0265
300	−0.4627	−1.0990	−0.0480	0.0256
305	−0.3100	−0.7362	−0.0368	0.0185
310	−0.2235	−0.5309	−0.0298	0.0375
315	−0.2458	−0.5837	−0.0360	0.0792
320	−0.0280	−0.0666	−0.0045	0.0171
325	−0.0266	−0.0632	−0.0045	0.0333
330	0.0947	0.2250	0.0170	0.0120
335	0.2030	0.4822	0.0381	0.0074
340	0.3095	0.7352	0.0603	0.0225
345	0.3563	0.8462	0.0713	0.0126
350	0.4126	0.9800	0.0842	0.0172
355	0.4170	0.9904	0.0861	0.0221
360	0.4137	0.9825	0.0857	0.0238

Data for Rough__high− Reynolds number = 27886.0886

theta [deg]	dp [in H2O]	cp []	cp*cos(th)d_th	dp +−[in H2O]
0	0.4267	1.0002	0.0873	0.0087
5	0.3973	0.9312	0.0810	0.0128
10	0.3538	0.8294	0.0713	0.0096
15	0.3388	0.7941	0.0669	0.0112
20	0.2097	0.4915	0.0403	0.0202
25	0.0346	0.0810	0.0064	0.0171
30	−0.0253	−0.0593	−0.0045	0.0214
35	−0.0871	−0.2043	−0.0146	0.0092
40	−0.3357	−0.7870	−0.0526	0.0173
45	−0.3611	−0.8465	−0.0522	0.0227
50	−0.4167	−0.9767	−0.0548	0.0107
55	−0.5095	−1.1942	−0.0598	0.0186
60	−0.6642	−1.5568	−0.0679	0.0191
65	−0.7657	−1.7948	−0.0662	0.0183
70	−0.7507	−1.7597	−0.0525	0.0184
75	−0.7709	−1.8070	−0.0408	0.0199
80	−0.7792	−1.8264	−0.0277	0.0225
85	−0.6043	−1.4164	−0.0108	0.0757
90	−0.5315	−1.2459	−0.0000	0.0123
95	−0.6554	−1.5363	0.0117	0.0301
100	−0.6486	−1.5204	0.0230	0.0112
105	−0.6028	−1.4129	0.0319	0.0164
110	−0.5914	−1.3862	0.0414	0.0222
115	−0.5459	−1.2796	0.0472	0.0134
120	−0.5166	−1.2108	0.0528	0.0136
125	−0.4394	−1.0300	0.0516	0.0149
130	−0.4589	−1.0756	0.0603	0.0131
135	−0.4584	−1.0746	0.0663	0.0190
140	−0.4648	−1.0895	0.0728	0.0162
145	−0.4922	−1.1537	0.0825	0.0117
150	−0.4817	−1.1291	0.0853	0.0086
155	−0.4672	−1.0951	0.0866	0.0151
160	−0.4295	−1.0068	0.0826	0.0238

165	−0.4192	−0.9827	0.0828	0.0129
170	−0.4361	−1.0223	0.0879	0.0278
175	−0.4227	−0.9908	0.0861	0.0115
180	−0.4173	−0.9781	0.0854	0.0138
185	−0.4313	−1.0110	0.0879	0.0143
190	−0.4455	−1.0442	0.0897	0.0196
195	−0.4788	−1.1222	0.0946	0.0174
200	−0.4733	−1.1094	0.0910	0.0129
205	−0.4837	−1.1338	0.0897	0.0117
210	−0.5011	−1.1746	0.0888	0.0116
215	−0.4825	−1.1310	0.0808	0.0106
220	−0.4883	−1.1445	0.0765	0.0107
225	−0.4940	−1.1580	0.0715	0.0090
230	−0.4863	−1.1398	0.0639	0.0180
235	−0.4566	−1.0702	0.0536	0.0180
240	−0.5197	−1.2181	0.0532	0.0084
245	−0.5596	−1.3116	0.0484	0.0167
250	−0.6336	−1.4851	0.0443	0.0228
255	−0.6255	−1.4662	0.0331	0.0474
260	−0.6454	−1.5129	0.0229	0.0356
265	−0.7004	−1.6418	0.0125	0.0170
270	−0.6485	−1.5201	0.0000	0.0221
275	−0.6858	−1.6076	−0.0122	0.0256
280	−0.6793	−1.5922	−0.0241	0.0124
285	−0.6851	−1.6059	−0.0363	0.0169
290	−0.6872	−1.6107	−0.0481	0.0216
295	−0.6258	−1.4668	−0.0541	0.0065
300	−0.5622	−1.3179	−0.0575	0.0118
305	−0.5065	−1.1871	−0.0594	0.0139
310	−0.3885	−0.9106	−0.0511	0.0187
315	−0.2942	−0.6895	−0.0425	0.0237
320	−0.1830	−0.4289	−0.0287	0.0214
325	−0.0023	−0.0053	−0.0004	0.0143
330	0.1452	0.3405	0.0257	0.0217
335	0.1474	0.3454	0.0273	0.0057
340	0.2405	0.5638	0.0462	0.0104
345	0.3555	0.8333	0.0702	0.0066
350	0.4164	0.9760	0.0839	0.0088
355	0.4339	1.0170	0.0884	0.0068
360	0.4265	0.9998	0.0872	0.0098

Drag coefficient

Object	Cd
Smooth_low	1.137
Rough__low	1.1013
Smooth_high	1.2264
Rough__high	1.0084

Year	Month	Day	Hour	Minute	Second
2007	5	17	17	16	31

=====================END OF OUTPUT FILE ====================

A.2 Experimental force balance results in tabular form

```
Drag coefficient results for smooth sphere
u [m/s]      F [N]     Re [ ]    Cd [ ]
12.2534     0.6605     26677     6.2992
16.5265     1.2577     35981     6.5945
20.8219     1.8550     45332     6.1272
25.1719     1.9065     54803     4.3089
Drag coefficient results for smooth sphere
u [m/s]      F [N]     Re [ ]    Cd [ ]
12.3132     0.7737     26808     7.3082
16.5487     1.2886     36029     6.7384
20.8747     1.7726     45447     5.8255
25.1865     1.8344     54835     4.1411
```

A.3 Matlab code for pressure distribution

```
%%%%%%%%%%%%%%%%%%%%%%%%%%%%%%%%%%%%%%%%%%%%%%%%%%%%%%%%%%%%%%%%%%%%%%%%%%%
%                MAE 440 Aerodynamics Laboratory Experiments              %
%                   Experiments conducted April 30th 2007                 %
%                        Niels Fuglede, 006020779                         %
%                                Project                                  %
%                                                                         %
%                Experiments on a smooth and rough sphere                 %
%                                                                         %
%%%%%%%%%%%%%%%%%%%%%%%%%%%%%%%%%%%%%%%%%%%%%%%%%%%%%%%%%%%%%%%%%%%%%%%%%%%
clear all, clf, close all, clc, format short
set(0,'DefaultFigureWindowStyle','docked')

%% Control color settings and save option
col=1;
save=1;
if col==1
    mrk =strvcat('r -','b -','g-','m-'); % Color
elseif col≠1
    mrk =strvcat('k -','k -','k--','k--'); % Black
end
 obj = ['Smooth_low '; 'Rough__low '; 'Smooth_high';'Rough__high']

%% Open outputfile
filename='fluidproject_out.txt';
fid=fopen(filename,'w');

%% Conversion factors, physical constants and dimensions
in2m=  0.0254;      % 1 inch = 0.0254 meters
nu   = 17.5e-6;     % [m^2/sec] kinematic viscosity
D    =  1.50*in2m;  % Sphere diameter

%% Load data
% Raw data
load data/p4l_mod.txt
load data/g4l.txt
load data/p4h.txt
load data/g4h.txt

% Initialise
N = length(p4l_mod);
n = 100;
x =zeros(n,N/n,4);
x1=zeros(n,N/n);
x2=zeros(n,N/n);
x3=zeros(n,N/n);
x4=zeros(n,N/n);

% Preferred data structure
k=0;
for j=1:N/n
    for i=1:n
        k=k+1;
        x1(i,j)=p4l_mod(k);
```

```
        x2(i,j)=g4l(k);
        x3(i,j)=p4h(k);
        x4(i,j)=g4h(k);
    end
end
clear ('p4l_mod','g4l','p4h','g4h')

x(1:n,1:N/n,1)=x1;
x(1:n,1:N/n,2)=x2;
x(1:n,1:N/n,3)=x3;
x(1:n,1:N/n,4)=x4;

clear ('x1','x2','x3','x4')

%% Drag calculations, mean free stream velocity and Reynolds number
% Initialise
dp_mean = zeros(N/n,4);
cp = zeros(N/n,4);
cp_cos_theta = zeros(N/n,4);
theta=linspace(0,360,N/n);
d_theta=5*pi/180;
c_d = zeros(1,4);

% Calculations
for k=1:4
   % mean pressure
   dp_mean(:,k)=mean(x(:,:,k));
   % stagnation pressure is taken as average of 0 and 360 degree measurement
   dp_stag(k)=(dp_mean(1,k)+dp_mean(end,k))/2;
   for i=1:N/n
       % Pressure coefficient is mean pressure/stagnation pressure
       cp(i,k)=dp_mean(i,k)./dp_stag(k);
       % Calculating pressure drag contribution for every angel
       cp_cos_theta(i,k)=cp(i,k)*cos(theta(i)*pi/180)*d_theta;
       % Summing up pressure contribution for every angel
       c_d(k) = c_d(k)+cp_cos_theta(i,k);
   end
   % 0 deg has been added twice (360 deg from n=73) => subtract last
   % contribution
   c_d(k) = c_d(k)-cp_cos_theta(N/n,k);
end

% Because of the symmetry of the cylinder
c_drag = 0.5*c_d;

%% Mean velocity and Reynolds number from 0 deg measurements
v_mean= zeros(1,4);
Re = zeros(1,4);
for k=1:4
   % Mean free stream velocity is calculated from stagnation pressure
   v_mean(k)=19.61*sqrt(dp_stag(k));
   % Reynolds number is calculated from the free stream velocity
   Re(k)=v_mean(k)*D./nu;
end

%% Uncertainty and error analysis
```

```
SD=zeros(N/n,4);
U =zeros(N/n,4);
for k=1:4
    % Standard deviation
    SD(:,k) = std(x(:,:,k));
end
U=2*SD;

%% Figures
figure(1)
    hold on
    mrk_er=['r';'b';'r';'b'];
for k=1:2
    errorbar(theta,cp(:,k),U(:,k),mrk_er(k,:))
end
    title('Low Speed','Fontsize',18,'Fontname','times')
    xlabel('\theta [deg]','Fontsize',16,'Fontname','times')
    ylabel('Cp_{mean} [ ]','Fontsize',16,'Fontname','times')
    legend('Smooth low ', 'Rough  low ',0)
    set(gca,'Fontsize',14,'Fontname','times')
    grid on
    axis([0,360,-2,1.5])
    set(gca,'XTick',[0 45 90 135 180 225 270 315 360])

figure(2)
    hold on
for k=3:4
    errorbar(theta,cp(:,k),U(:,k),mrk_er(k,:))
end
    title('High Speed','Fontsize',18,'Fontname','times')
    xlabel('\theta [deg]','Fontsize',16,'Fontname','times')
    ylabel('Cp_{mean} [ ]','Fontsize',16,'Fontname','times')
    legend('Smooth high','Rough  high',0)
    set(gca,'Fontsize',14,'Fontname','times')
    grid on
    axis([0,360,-2,1.5])
    set(gca,'XTick',[0 45 90 135 180 225 270 315 360])

figure(3)
    hold on
for k=[1,3]
    plot(theta,cp(:,k),mrk(k,:))
end
    title('Low and High Speed of smooth sphere','Fontsize',18,'Fontname','times')
    xlabel('\theta [deg]','Fontsize',16,'Fontname','times')
    ylabel('Cp_{mean} [ ]','Fontsize',16,'Fontname','times')
    legend('Smooth low ','Smooth high',0)
    set(gca,'Fontsize',14,'Fontname','times')
    grid on
    axis([0,360,-2,1.5])
    set(gca,'XTick',[0 45 90 135 180 225 270 315 360])

figure(4)
    hold on
for k=[2,4]
    plot(theta,cp(:,k),mrk(k,:))
```

```
end
    title('Low and High Speed of rough sphere','Fontsize',18,'Fontname','times')
    xlabel('\theta [deg]','Fontsize',16,'Fontname','times')
    ylabel('Cp_{mean} [ ]','Fontsize',16,'Fontname','times')
    legend('Rough low ','Rough high',0)
    set(gca,'Fontsize',14,'Fontname','times')
    grid on
    axis([0,360,-2,1.5])
    set(gca,'XTick',[0 45 90 135 180 225 270 315 360])

%% Printout
for k=1:4
    disp(['Data for ',obj(k,:),'- Reynolds number = ',num2str(Re(k))])
    disp('----------------------------------------------------------------')
    disp('    theta        dp        cp   cp*cos(th)d_th  dp +-')
    disp('----------------------------------------------------------------')
    disp([theta', dp_mean(:,k),cp(:,k),cp_cos_theta(:,k),U(:,k)])

    fprintf(fid,['\nData for ',obj(k,:),'- Reynolds number = ',num2str(Re(k)),'\n']);
    fprintf(fid,'----------------------------------------------------------------\n');
    fprintf(fid,'theta [deg] dp [in H2O] cp [] cp*cos(th)d_th  dp +-[in H2O]\n');
    fprintf(fid,'----------------------------------------------------------------\n');
    fprintf(fid,'%7.0f    %7.4f   %7.4f    %7.4f   %7.4f\n',[theta', dp_mean(:,k),cp(:,k),cp_cos_t
end

disp(['Drag coefficient'])
disp(['------------------------'])
disp(['Object        Cd   '])
disp(['------------------------'])

fprintf(fid,['\nDrag coefficient\n']);
fprintf(fid,['------------------------\n']);
fprintf(fid,['Object        Cd   \n']);
fprintf(fid,['------------------------']);

for k=1:4
    disp([obj(k,:),'   ' num2str(c_drag(k))])
    fprintf(fid,'\n%9s  %7.4f',[obj(k,:),'   ' num2str(c_drag(k))]);
end
%% Save figures
if save==1
    % In color
    if col==1
        print -f1 -depsc '../mfigc/lowspeedc.eps'
        print -f2 -depsc '../mfigc/highspeedc.eps'
        print -f3 -depsc '../mfigc/smoothc.eps'
        print -f4 -depsc '../mfigc/golfc.eps'
       % print -f5 -depsc '../mfigc/maxturvelc.eps'
       % print -f6 -depsc '../mfigc/momthc.eps'
       % print -f7 -depsc '../mfigc/yhalfc.eps'
    % In black and white
    elseif col≠1
        saveas(1,'../mfig/lowspeed.eps','eps')
        saveas(2,'../mfig/highspeed.eps','eps')
        saveas(3,'../mfig/smooth.eps','eps')
        saveas(4,'../mfig/golf.eps','eps')
```

```
     %   saveas(5,'../mfig/maxturvel.eps','eps')
     %   saveas(6,'../mfig/momth.eps','eps')
     %   saveas(7,'../mfig/yhalf.eps','eps')
    end
end

%% End of script
disp('=====================END OF SCRIPT====================');
fprintf(fid,' \n  Year     Month   Day     Hour   Minute  Second\n');
fprintf(fid,'%6.0f  %6.0f  %6.0f  %6.0f  %6.0f  %6.0f\n',[fix(clock)]);
fprintf(fid,'\n=====================END OF OUTPUT FILE ====================');
fclose(fid);
```

A.4 Matlab code for one dimensional balance

```
%%%%%%%%%%%%%%%%%%%%%%%%%%%%%%%%%%%%%%%%%%%%%%%%%%%%%%%%%%%%%%%%%%%%%%%%%%%%
%                MAE 440 Aerodynamics Laboratory Experiments               %
%                   Experiments conducted April 30th 2007                  %
%                        Niels Fuglede, 006020779                          %
%                                Project                                   %
%                                                                          %
%                Experiments on a smooth and rough sphere                  %
%                                                                          %
%%%%%%%%%%%%%%%%%%%%%%%%%%%%%%%%%%%%%%%%%%%%%%%%%%%%%%%%%%%%%%%%%%%%%%%%%%%%
clear all, clf, close all, clc, format short
set(0,'DefaultFigureWindowStyle','docked')

%% Open outputfile
filename='fluidprojectforce_out.txt';
fid=fopen(filename,'w');

%% Constants
lb2kg=0.45359237; % 1 pound = 0.45359237 kilograms
in2m =0.0254;     % 1 inch = 0.0254 meters
rho = 1.2250;     % [kg/m^3] from page 965 in Fundamentals of Aerodynamics
g = 9.81;         % [m/s^2]
nu= 17.5e-6;      % [m^2/sec] kinematic viscosity
D =  1.50*in2m;   % Sphere diameter

%% Calibration Data
cal_F=[0.593, 1.593,2.593,3.593]*lb2kg*g; % [Newton]
cal_V=[0.209,0.673,1.22,1.467];

%% Calibration using least-squares fit - [Volt/Newton]
lin_reg = polyfit(cal_F,cal_V,1);
R_cal = corrcoef(cal_F,cal_V)
a = lin_reg(1) % Slope [volt/Newton]
b = lin_reg(2) % Intersept [volt]

disp('Caibration constants in y=a*x+b')
disp('     a         b                ')
disp([a b])

%% Calcultation of drag coefficients
dp_p=[0.409,0.744,1.181,1.726];
V_p=[0.0520,0.110,0.168,0.173];

dp_g=[0.413,0.746,1.187,1.728];
V_g=[0.063,0.113,0.160,0.166];

%% Velocity, force, Re, drag coefficient
A=(D/2)^2*pi;
u_p=19.16*sqrt(dp_p);
u_g=19.16*sqrt(dp_g);

F_p=1/a.*V_p;
F_g=1/a.*V_g;
```

```
Re_p = D*u_p./nu;
Re_g = D*u_g./nu;

Cd_p=F_p./(0.5.*rho.*u_p.^2.*A);
Cd_g=F_g./(0.5.*rho.*u_g.^2.*A);

disp('Drag coefficient results for smooth sphere')
disp('u [m/s]    F [N]    Re [ ]   Cd [ ]')
disp([u_p' F_p' Re_p' Cd_p'])
fprintf(fid,'Drag coefficient results for smooth sphere\n');
fprintf(fid,'u [m/s]       F [N]      Re [ ]     Cd [ ]\n');
fprintf(fid,'%7.4f    %7.4f   %7.0f    %7.4f \n',[u_p' F_p' Re_p' Cd_p']');

disp('Drag coefficient results for rough sphere')
disp('u [m/s]    F [N]    Re [ ]   Cd [ ]')
disp([u_g' F_g' Re_g' Cd_g'])
fprintf(fid,'Drag coefficient results for smooth sphere\n');
fprintf(fid,'u [m/s]       F [N]      Re [ ]     Cd [ ]\n');
fprintf(fid,'%7.4f    %7.4f   %7.0f    %7.4f \n',[u_g' F_g' Re_g' Cd_g']');
%% Drag coefficients from force balance
figure(1)
plot(cal_F,cal_V,'+');
title('Force calibration and linear regression','Fontsize',18,'Fontname','times')
xlabel('Force [Newton]','Fontsize',16,'Fontname','times');
ylabel('Output [Volt]','Fontsize',16,'Fontname','times');
legend('calibration data',4)
set(gca,'Fontsize',14,'Fontname','times')
axis([0,16,0,1.6])
grid on
% print -f1 -depsc '../mfigc/forcecalibration.eps'

%% Drag coefficients from force balance
figure(2)
plot(Re_p,Cd_p,'r-+',Re_g,Cd_g,'b-+');
title('Drag coefficient as a function of Reynolds number','Fontsize',18,'Fontname','times')
xlabel('Re [ ]','Fontsize',16,'Fontname','times');
ylabel('Cd [ ]','Fontsize',16,'Fontname','times');
legend('Smooth sphere','Rough sphere',3)
set(gca,'Fontsize',14,'Fontname','times')
grid on
% print -f2 -depsc '../mfigc/dragfromforce.eps'
fclose(fid);
```